International Journal of Engineering Science 123 (2018) 73–80

Contents lists available at ScienceDirect

International Journal of Engineering Science

journal homepage: www.elsevier.com/locate/ijengsci

On simple scaling laws for pumping fluids with electrically-charged particles

Tarek I. Zohdi

Department of Mechanical Engineering, UC Berkeley Will C. Hall Family Endowed Chair in Engineering Chair, UC Berkeley Comp. and Data Science and Engineering Program, 6117 Etcheverry Hall, UC, Berkeley, CA 94720-1740, USA

ARTICLE INFO

Article history:
Received 8 November 2017
Accepted 13 November 2017

Keywords:
Complex fluids
Electric fields
Charged particles

ABSTRACT

As 3D printing has matured, the use of more complex materials has increased. In particular, particle-functionalized inks are now relatively wide-spread. Because of the desire to have faster throughput for industrial-scale printing, electrically-driven flow of such materials is being pursued. In many cases, such fluids consist of an electrically-neutral base solvent with embedded charged particles. As one increases the volume fraction of particles, two effects effects arise: (1) an increase in effective overall viscosity fluid and (2) an increase in the induced electrical force that can be applied. In the present analysis, the governing equations for the required pressure gradient in a pipe to move the fluid with a constant flow rate are derived. A key nondimensional scaling ratio governing the relative contribution of electrical and viscous fluid forces to the system behavior is also identified. Numerical examples are provided to illustrate the results.

© 2017 Elsevier Ltd. All rights reserved.

1. Introduction

In a variety of industries involving printed electronics, new types of particle-laden materials are being developed and utilized. In the development of such materials, the basic philosophy is to select material combinations to produce desired aggregate responses upon deposition onto a substrate. Oftentimes, such materials start in a fluidized form comprised of particles in a solvent, forming a viscous “ink”. However, because of the increasing demands for faster throughput and industrial-scale printing of complex particle-laden materials, the determination of accurate pumping pressures needed to move such fluids through delivery piping systems is critical (Fig. 1).

One approach to increase the throughput is to utilize electrical fields to drive the flows whenever possible, which is often referred to as electrical injet printing or electrohydrodynamic printing. This is particularly useful for fluids that contain electromagnetically-sensitive particles. “Electrical fluids” are typically functionalized by embedding charged or electrically sensitive particles in a neutral fluid. Because of 3D-printing, there has been an increased interest in this class of materials because of so-called electrically-functionalized inks (“e-inks”), driven by the printed electronics industry. Electrical inkjet printing is particularly attractive due to its high throughput, however, this comes with increases in the overall viscosity of the fluid. Electrohydrodynamic printing has also been proposed to increase the resolution beyond the limits of inkjet printing, achieving a line resolution as small as 700 nm (Park et al., 2008, 2007). There are a variety of related high-throughput industrial techniques, and we refer the reader to the surveys found in Martin (2009, 2011), as well as the works of Ahmad, Rasekh, and Edirisinghe (2010), Samarasinghe, Pastoriza-Santos, Edirisinghe, Reece, and Liz-Marzan (2006),

E-mail address: zohdi@berkeley.edu

https://doi.org/10.1016/j.ijengsci.2017.11.003
0020-7225/© 2017 Elsevier Ltd. All rights reserved.

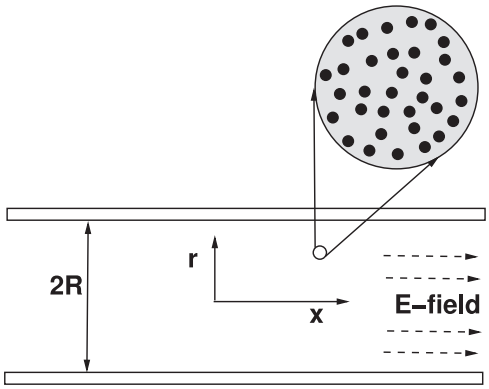

Fig. 1. Flow of a particle-laden through a pipe in the presence of an applied electric field.

Choi et al. (2010a), Choi, Stassi, Pisano, and Zohdi (2010b), Choi et al. (2012), Choi, Pisano, and I. (2013) and Demko, Cheng, and Pisano (2010) and Demko, Choi, Zohdi, and Pisano (2012).

The main objective of this work is to develop a relatively simple model for the pressure gradients needed to move fluids containing charged particles as a function of (1) the applied electric field, (2) the volume fraction of added particles, (3) the pipe radius, (4) the volumetric flow rate, (5) the fluid-induced intensity of the shear stress at the pipe wall and (6) the base fluid viscosity. As mentioned previously, this has become increasingly more important to 3D printing industry, which is attempting to rapidly print complex electrical inks ("e-inks"), where the embedded particles endow the cured printed materials with overall (mechanical, electrical, thermal, magnetic, etc.) properties that the pure solvent (particle-free ink) alone does not possess. An overall objective of the analysis is to develop semianalytical expressions that can help guide analysts who are designing manufacturing systems involving particle-laden e-inks. Theoretically speaking, one could attempt a large-scale CFD analysis, however, for accurate direct numerical simulation of particle-laden continua, the spatial discretization grids must be extremely fine, with several thousand numerical unknowns needed per particle length-scale. Furthermore, extremely fine time-discretization is required. Thus, for even a small system with several hundred-thousand particles, a proper discretization would require several billion numerical unknowns (see, for example, Avci and Wriggers, 2012; Leonardi, Wittel, Mendoza, and Herrmann, 2014; Onate et al., 2014; Zohdi, 2014; Zohdi and Wriggers, 2008). Although such simulations are possible in high-performance computing centers, their usefulness for rapid daily design analysis for e-inks and related materials is minimal. *Therefore, in this paper we seek to develop simplified approaches.*This work presents analytical calculations to predict the pressure required to pump a suspension of rigid, charged particles in an idealized non-conducting fluid through a pipe of circular cross-section, under the assumption that the flow is uni-directional and fully developed. It first arrives at an analytical modification of Poiseulle flow through a pipe. The analysis assumes the suspension can simply treated as a homogenous fluid with an effective viscosity μ^*. This is a simplification, in order to develop useful and practical analytical results, without having to resort to computationally-intensive numerical methods which seek to calculate μ^* from detailed accounting of the micro-scale hydrodynamic interactions between particles in a suspension.

Remark. The upcoming analysis of a fluid seeded with charged particles exposed to an external electric field simplifies the fundamental aspects of electrokinetic flows, with the objective being to develop simple scaling laws for such systems. Readers interested in more detailed analyses can consult books such (Probstein, 2003), specifically on electric double layers and hydrodynamics of charged particles. In the present simplified analysis, the bulk mixture is charged (idealized as a neutral fluid with embedded charged particles). Implicitly, in is assumed that the particles are on the order of 10 nm, since charged mixtures with particles at length-scales larger than that are unlikely to sustain their charge. This is because the counter-ions in the carrier fluid will be attracted to the surface of particles. This effect leads to the formation of thin electric double layers shielding the charge of the particles. Therefore, the effective force felt by the particles due to an external field will be significantly suppressed. Furthermore, we assume that the charged particles remain uniformly spaced, and that any possible repulsive electrostatic force between the particles, does not have they enough time or strength to force the particles to migrate towards the walls very quickly. It is also assumed that the electric force is proportional to the volume fraction of particles, which is accurate at moderate volume fractions, but which is questionable at larger volume fractions, where electrical interactions between particles should be resolved.

2. Flow of an electrical-fluid through a pipe of radius *R*

We consider a fluid that is capable of carrying an electrical charge. Taking an annular element and summing the pressure and shear forces in the axial direction, along with uniform electrical body force, yields

$$-\frac{\partial P}{\partial x}+\frac{1}{r}\frac{\partial (r\tau)}{\partial r}+f_e^*=0 \Rightarrow \frac{1}{r}\frac{\partial (r\tau)}{\partial r}=\frac{\partial P}{\partial x}-f_e^*. \tag{2.1}$$

Integrating yields

$$\tau = \frac{r}{2}\left(\frac{\partial}{\partial x} - f_e^*\right) + \frac{C_1}{r} = \mu^* \frac{\partial v}{\partial r}. \tag{2.2}$$

Integrating again yields

$$v(r) = \frac{1}{\mu^*}\left(\frac{r^2}{4}\left(\frac{\partial P}{\partial x} - f_e^*\right) + C_1 lnr\right) + C_2. \tag{2.3}$$

$v(r=0)$ must be finite, thus $C_1 = 0$, and $v(r=R) = 0$ yields

$$v(r) = -\frac{R^2}{4\mu^*}\left(\frac{\partial P}{\partial x} - f_e^*\right)\left(1 - \left(\frac{r}{R}\right)^2\right) \tag{2.4}$$

Note that $v(r)$ is a maximum where

$$\frac{\partial v}{\partial r} = 0 = \frac{R^2}{4\mu^*}\left(\frac{\partial P}{\partial x} - f_e^*\right)\frac{2r}{R^2}, \tag{2.5}$$

which is at $r = 0$. Thus,

$$v_{max} = v(r=0) = -\frac{R^2}{4\mu^*}\left(\frac{\partial P}{\partial x} - f_e^*\right) \Rightarrow v(r) = v_{max}\left(1 - \left(\frac{r}{R}\right)^2\right) \tag{2.6}$$

If we assume that the flow rate is constant

$$Q = Q_o = \int_A v\, dA = \frac{\pi v_{max} R^2}{2} \Rightarrow v_{max} = \frac{2Q_o}{\pi R^2}, \tag{2.7}$$

and we obtain

$$v(r) = \frac{2Q_o}{\pi R^2}\left(1 - \left(\frac{r}{R}\right)^2\right) \tag{2.8}$$

The stress at becomes

$$\tau(r) = \mu^* \frac{\partial v(r)}{\partial r} = -\frac{4\mu^* Q_o r}{\pi R^4}. \tag{2.9}$$

The stress at the wall becomes

$$\tau_w = -\tau(r=R) = \frac{2\mu^* v_{\max}}{R} = \frac{4\mu^* Q_o}{\pi R^3}. \tag{2.10}$$

We have the following observations: (a) Increasing μ^* or Q_o increases the stress at the wall (τ_w) and (b) Decreasing R increases the stress at the wall (τ_w). In the remaining analysis, we will assume steady flow, the particles are not elongated and that they are well distributed within the base fluid.

3. Pressure gradients

The previous expressions allow us to correlate the pressure applied to a volume of particle-laden to allow it to move as a constant flow rate. By performing a force balance, we have in the positive x-direction (assuming steady flow, no acceleration)

$$(-(P + \Delta P) + P)\pi R^2 - \tau_w 2\pi R \Delta x + f_e^* \pi R^2 \Delta x = 0, \tag{3.1}$$

where x is the coordinate along the length of the pipe and Δx is the differential length, leading to

$$-\Delta P = \mu^* \frac{4Q_o}{\pi^2 R^5} 2\pi R \Delta x - f_e^* \Delta x = 0, \quad \rightarrow -\frac{\Delta P}{\Delta x} = -\frac{\partial P}{\partial x} = \frac{8\mu^* Q_o}{\pi R^4} - f_e^*, \tag{3.2}$$

where we used the expression for $v_{\max}$ and where the effective viscosity is a function of the volume fraction of particles, $\mu^* = \mu^*(\nu_p)$. An explicit relation for $\mu^*(\nu_p)$ will be given shortly. Solving for the pressure gradient yields

$$-\frac{\Delta P}{\Delta x} = -\frac{\partial P}{\partial x} = \underbrace{\frac{8\mu^*}{\pi R^4}}_{C} Q_o - f_e^* \stackrel{\text{def}}{=} C Q_o - f_e^*. \tag{3.3}$$

If we fix the flow rate Q_o, the multiplier C and f_e^* identify the pressure gradient needed to achieve a flow rate Q_o. For small pipes this can be a problem, as indicated by the R^4 term in the denominator.

4. Decomposition of the electrical force

One can integrate the total electromotive force per unit volume as

$$f_e^* \stackrel{\text{def}}{=} \langle f_e(\boldsymbol{x})\rangle_V \stackrel{\text{def}}{=} \frac{1}{V}\int_V f_e\, dV = \frac{1}{V}\left(\int_{V_f} f_{e-f}\, dV + \int_{V_p} f_{e-p}\, dV\right) = \nu_f\langle f_{e-f}\rangle_{\Omega_f} + \nu_p\langle f_{e-p}\rangle_{\Omega_p}. \tag{4.1}$$

Decomposing the electrical force into the electric field, E and the charge per unit volume, λ, yields

$$f_e^* = \nu_f\langle \lambda_f E\rangle_{\Omega_f} + \nu_p\langle \lambda_p E\rangle_{\Omega_p}. \tag{4.2}$$

Assuming that the base fluid carries no charge, that the electric field E is uniform and that the charge in each particle is uniform yields

$$f_e^* = \nu_p\langle \lambda_p E\rangle_{\Omega_p} = \nu_p\lambda_p E. \tag{4.3}$$

Thus, we have

$$-\frac{\partial P}{\partial x} = \underbrace{\frac{8\mu^*}{\pi R^4}}_{C} Q_o - f_e^* \stackrel{\text{def}}{=} CQ_o - \nu_p\lambda_p E. \tag{4.4}$$

The ratio of the electrical force to the viscous force is

$$\Lambda \stackrel{\text{def}}{=} \frac{\pi R^4 \nu_p \lambda_p E}{8\mu^* Q_o}. \tag{4.5}$$

The effective viscosity is a function of ν_p, which we discuss next.

5. Models for effective properties of particle-laden fluids

A key component of the analysis requires the characterization of the effective properties of a particle-laden fluid as a function of the volume fraction of particles and the baseline (interstitial) fluid properties. The density of the particle-laden fluid is actually an "effective density", since it actually is a mixture of materials (particles and interstitial fluid). Effective properties are defined through volume averages. For example, the effective density of the mixture is

$$\rho^* \stackrel{\text{def}}{=} \langle \rho(\boldsymbol{x})\rangle_V \stackrel{\text{def}}{=} \frac{1}{V}\int_V \rho(\boldsymbol{x})\, dV = \frac{1}{V}\left(\int_{V_f} \rho_f\, dV + \int_{V_p} \rho_p\, dV\right) = \nu_f\rho_f + \nu_p\rho_p \tag{5.1}$$

where ν_f and ν_p are the volume fractions of the fluid and particles, respectively. The volume fractions have to sum to unity: $\nu_f + \nu_p = 1 \Rightarrow \nu_f = 1 - \nu_p$. Similar approaches can be used to calculate various types of properties, such as the effective viscosity. However, to calculate it is somewhat more complicated, since it requires one to estimate the interaction between the constituents. There are a number of models which provide expressions for the effective viscosity of the fluid containing particles. One of the first models for the effective viscosity of such fluids was developed in 1906 by Einstein (1906). It reads as

$$\mu^* = \mu_f(1 + 2.5\nu_p), \tag{5.2}$$

where μ^* is the effective viscosity, μ_f is the viscosity of the fluid and ν_p is the volume fraction of particles. This expression is accurate only for low volume fractions of particles. A more accurate approximation, *in fact a strict, rigorous, lower bound* (accurate up to approximately $\nu_p = 20\%$, which is sufficient for most applications of interest) can be derived from the well-known Hashin and Shtrikman bounds (Hashin and Shtrikman, 1962, 1963, and Hashin, 1983) bounds in solid mechanics. Specifically, for linearized elasticity applications, for isotropic materials with isotropic effective (mechanical) responses, the Hashin–Shtrikman bounds (for a two-phase material) are as follows for the effective bulk modulus (κ^*)

$$\kappa^{*,-} \stackrel{\text{def}}{=} \kappa_1 + \frac{\nu_2}{\frac{1}{\kappa_2-\kappa_1} + \frac{3(1-\nu_2)}{3\kappa_1+4\mu_1}} \le \kappa^* \le \kappa_2 + \frac{1-\nu_2}{\frac{1}{\kappa_1-\kappa_2} + \frac{3\nu_2}{3\kappa_2+4\mu_2}} \stackrel{\text{def}}{=} \kappa^{*,+} \tag{5.3}$$

and for the effective shear modulus (G^*)

$$G^{*,-} \stackrel{\text{def}}{=} G_1 + \frac{\nu_2}{\frac{1}{G_2-G_1} + \frac{6(1-\nu_2)(\kappa_1+2G_1)}{5G_1(3\kappa_1+4G_1)}} \le G^* \le G_2 + \frac{(1-\nu_2)}{\frac{1}{G_1-G_2} + \frac{6\nu_2(\kappa_2+2G_2)}{5G_2(3\kappa_2+4G_2)}} \stackrel{\text{def}}{=} G^{*,+}, \tag{5.4}$$

where κ_1 (usually the matrix material) and κ_2 (usually the particulate material) are the bulk moduli and G_1 and G_2 are the shear moduli of the respective phases ($\kappa_2 \ge \kappa_1$ and $G_2 \ge G_1$), and where ν_2 is the second phase volume fraction. Such bounds are the tightest possible on isotropic effective responses, with isotropic two phase microstructures, where only the volume fractions and phase contrasts of the constituents are known (see Hashin, 1983 for a discussion on the optimality of such bounds). Note that no geometric or statistical information is required for the bounds. For an authoritative review of the general theory of random heterogeneous media see Torquato (2002). One can take the limit of the particle phase becoming

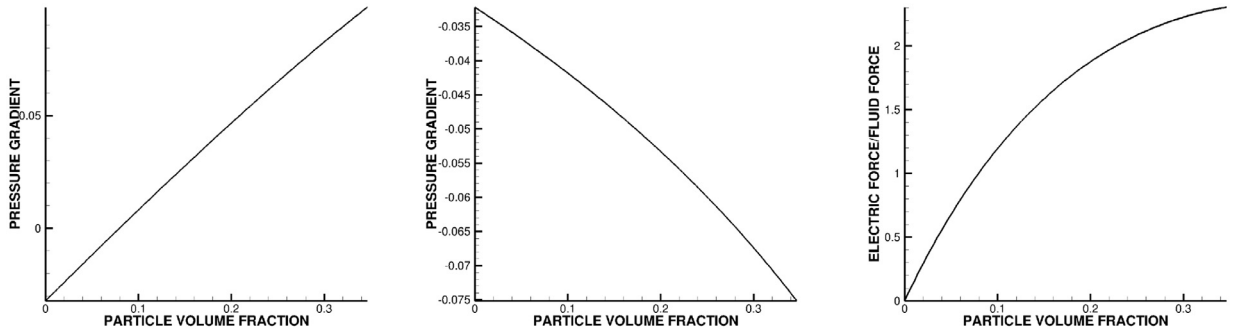

Fig. 2. LEFT: the pressure gradient needed ($\frac{\Delta P}{\Delta x}$) as a function of volume fraction of v_p with an electric field present. MIDDLE: the pressure gradient needed ($\frac{\Delta P}{\Delta x}$) as a function of volume fraction of v_p with no electric field present. RIGHT: the ratio of the electric force to the fluid forces (Λ).

rigid, i.e. the bulk and shear moduli tending towards infinity, $\kappa_2 = \kappa_p \to \infty$ and $G_2 = \mu_p \to \infty$, signifying that the particles are much stiffer than the interstitial fluid, while simultaneously specifying that the interstitial fluid is incompressible, i.e. $\kappa_1/G_1 = \kappa_f/\mu_f \to \infty$ with G_1 being finite. This yields,

$$\mu^* \geq \mu^{*,-} = \mu_f \left(1 + 2.5 \frac{v_p}{1 - v_p} \right). \tag{5.5}$$

Eq. (5.5) represents the tightest known lower bound on the effective viscosity of a two-phase material comprised of rigid particles in a surrounding incompressible fluid. The bound recapture the Einstein result in the $v_p \to 0$ limit, but is a rigorous lower bound at significant v_p. *This rigorous lower bound* is extremely accurate up to approximately 20 % volume fraction. These bounds have been tested in the numerical analysis literature repeatedly, for example against direct Finite Element calculations found in Zohdi and Wriggers (2008). We refer the reader to Kachanov and Abedian (2015) for more in depth analysis on the effective viscosity of particle-laden fluids see Sevostianov and Kachanov (2012) for the analysis of the proper application of the non-interaction and the "dilute limit" approximations and for detailed discussions on the isotropic and anisotropic viscosity of suspensions containing particles of diverse shapes and orientations. It is important to emphasize that (Kachanov & Abedian, 2015) is accurate for up to 25–30 % in case of spherical particles. Furthermore, Kachanov and Abedian (2015) covers other shapes, including, importantly, mixtures of diverse shapes. Of course, one can one employ formulas such as in Kachanov and Abedian (2015) for more accuracy, however, because the Hashin–Strikman expression is a strict lower bound, $\mu^{*,-} \leq \mu^*$, we consequently generate a strict lower bound for the pressure gradient

$$-\frac{\partial P}{\partial x} \geq \underbrace{\frac{8\mu^{*,-}}{\pi R^4}}_{C^-} Q_o - f_e^* \stackrel{\text{def}}{=} C^- Q_o - v_p \lambda_p E \tag{5.6}$$

and a strict upper bound on the ratio of the electrical force to the viscous force

$$\Lambda \leq \frac{\pi R^4 v_p \lambda_p E}{8\mu^{*,-} Q_o}. \tag{5.7}$$

6. Trends

We plotted the pressure gradient as a function of v_p, with the following parameters:[1] (a) viscosity, $\mu_f = 0.01\,\text{Pa} - \text{s}$, (b) fluid density: $\rho_f = 1000\,\text{kg/m}^3$, (c) particle density: $\rho_p = 5000\,\text{kg/m}^3$, (d) flow rate: $Q_o = 0.000001\,\text{m}^3/\text{s}$, (e) pipe radius: $R = 0.001\,\text{m}$, and (f) electric force: $qE = 500,000$. At approximately 8 % volume fraction, the required pressure gradient to maintain the specified Q_o crosses from being negative (as it would be if there is no electric field). Approximately at this volume fraction, no pressure gradient is needed. As a baseline for comparison, Fig. 2 shows the pressure gradient needed with no electric field. This steadily increases with particle volume fraction (approximately 2.4 times the pressure gradient is needed for a 35 % volume fraction fluid that for a pure baseline fluid (zero volume fraction). Due to the increase in the particle volume fraction, the viscosity increases, thus decreasing the Reynolds number. The point of this example was not to illustrate an all encompassing parameter set, but simply to show the explicit dependency of the pressure gradient on the presence of secondary particles, with and without an electric field. Other parameter sets can be easily simulated.

7. Summary and extensions

In summary, as one increases the volume fraction of particles in an electrically-functionalized fluid, two effects effects arise: (1) an increase in effective overall viscosity fluid and (2) an increase in the induced electrical force that can be applied.

[1] For reference, the viscosity of water is $\mu_f = 0.001\,\text{Pa} - \text{s}$ and for honey, $\mu_f = 1\,\text{Pa} - \text{s}$.

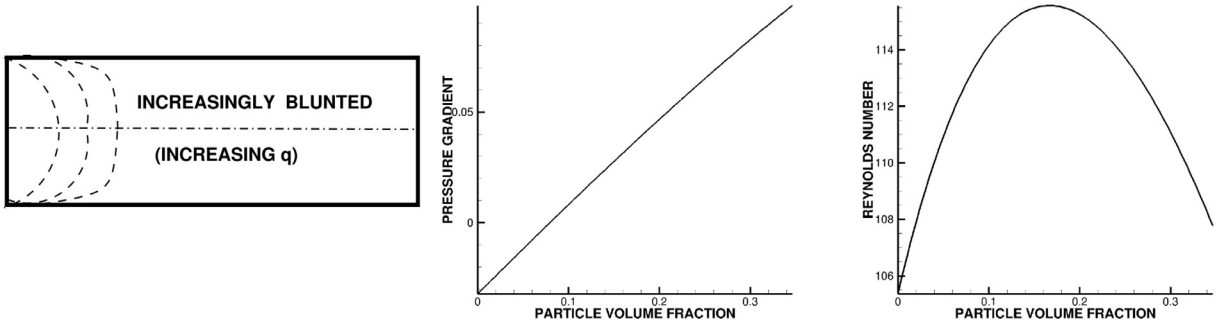

Fig. 3. LEFT: progressive blunting of the velocity profile with increasing q. MIDDLE: the pressure gradient needed ($\frac{\Delta P}{\Delta x}$) as a function of volume fractions of ν_p. RIGHT: the resulting Reynolds number.

Because the presence of particles increases the overall viscosity of the fluid, the pressure gradients needed to pump such fluids through pipes at a nominal flow rate can increase dramatically. The use of an electric field, if the particles are charged, can dramatically decrease the pressure gradients needed to achieve a predetermined flow rate. This paper developed the governing equations for the required pressure gradient in a pipe to move the fluid with a constant flow rate in the presence of an electric field. A nondimensional ratio governing the relative contribution of electrical and viscous fluid forces to the system behavior was identified and numerical examples are provided to illustrate the results. The nondimenional expression explicitly correlates the dependency of the pressure gradient and the applied electric field to the particle volume fraction. To obtain more detailed information, for example on the flow profile as a function of the input parameters, the model can be extended further rather easily. For example, consider we again idealized pipe with a circular cross-section of area $A = \pi R^2$, with a velocity profile given by a phenomenological extension:

$$v = v_{\max}\left(1 - \left(\frac{r}{R}\right)^q\right), \tag{7.1}$$

where q is now considered a variable. For fully developed laminar flow, $q = 2$, while for increasing q one characterizes, phenomenologically, progressively turbulent flow ($q \geq 2$). The shear stress is given by

$$\tau = \mu^* \frac{\partial v}{\partial r} = -\frac{\mu^* v_{\max} q}{R}\left(\frac{r}{R}\right)^{q-1}, \tag{7.2}$$

where μ^* is the effective viscosity of the particle-laden fluid. We assume that the overall flow rate is assumed constant, thus $Q = \int_A v\, dA = Q_o$. One can show that

$$v_{\max} = \frac{Q_o(q+2)}{Aq} = \frac{Q_o(q+2)}{\pi R^2 q}. \tag{7.3}$$

The stress at the wall becomes

$$\tau_w = -\tau(r = R) = \frac{\mu^* v_{\max} q}{R} = \frac{\mu^* Q_o (q+2)}{\pi R^3}. \tag{7.4}$$

We observe that as q increases the stress at the wall (τ_w) increases and that increasing q leads to an increasingly more blunted flow profile. As before, by performing a force balance we have in the positive x-direction (assuming steady flow, no acceleration) we obtain an expression for the pressure gradient yields

$$-\frac{\Delta P}{\Delta x} = -\frac{\partial P}{\partial x} = \underbrace{\frac{2\mu^*(q+2)}{\pi R^4}}_{C} Q_o - f_e^* \stackrel{\text{def}}{=} C Q_o - f_e^*. \tag{7.5}$$

This generalization of the classical Poiseuille solution for fully developed flow in a pipe (assuming the velocity depends on some undetermined power q instead of the standard parabolic dependence. We solve for q next. However, in general, q is a function of the Reynolds number. This case will be considered next. As the Reynolds number increases, the velocity profile will change from a quadratic ($q = 2$) to a more blunted profile ($q > > 2$), which represents, phenomenologically, turbulent (inertia-dominated) behavior (Fig. 3). The effect of a changing profile is described by representing q by a linear function of the centerline Reynolds' number ($\mathcal{R}_{ec}$)

$$q = q(\mathcal{R}_{ec}) = c_1 \mathcal{R}_{ec} + c_2, \tag{7.6}$$

where $\mathcal{R}_{ec} = \frac{\rho^* v_{\max} 2R}{\mu^*}$ and c_1 and c_2 are constants. Models of this type, linking the profile exponent (q) to the centerline Reynolds' number ($\mathcal{R}_{ec}$), are quite well-established, for example, see Hinze (1975). Usually, $0 \leq c_1 < < 1$ and $c_2 \approx 2$, and in the limit we have, for $c_1 = 0$ and $c_2 = 2$, laminar flow ($q = 2$). For the general case, combining Eq. (7.3) with Eq. (7.6) and the definition of the centerline Reynolds' number, we obtain a quadratic relationship for q,

$$q^2 - (\gamma^* + c_2)q - 2\gamma^* = 0, \tag{7.7}$$

where $\gamma^* = \frac{2c_1 Q_o \rho^*}{\pi R \mu^*}$, where ρ^* is the effective density and μ^* is the effective viscosity. This quadratic relationship can be solved in closed form for q to yield[2]

$$q(\mathcal{R}_{ec}) = \frac{1}{2}\left((\gamma^* + c_2) \pm \sqrt{(\gamma^* + c_2)^2 + 8\gamma^*}\right). \tag{7.8}$$

The larger root is the physically correct choice (since the smaller root can become negative). We further observe that $q(\mathcal{R}_{ec})$ is a function of R^{-1} and decreasing R increases q, for fixed Q_o. Using the effective properties, we have an expression for the velocity profile exponent

$$q(\mathcal{R}_{ec}(\mu^*, \rho^*), \gamma^*) = \frac{1}{2}\left((\gamma^* + c_2) \pm \sqrt{(\gamma^* + c_2)^2 + 8\gamma^*}\right). \tag{7.9}$$

Consequently, the pressure gradient's dependency on the volume fraction of particles can be written as

$$-\frac{\partial P}{\partial x} = \frac{2(\mu_f(1 + 2.5\frac{\nu_p}{1-\nu_p}))(q(\mathcal{R}_{ec}(\mu^*, \rho^*), \gamma^*) + 2)}{\pi R^4} Q_o - \nu_p \lambda_p E \stackrel{\text{def}}{=} C^* Q_o - \nu_p \lambda_p E, \tag{7.10}$$

where $C^* = C^*(Q_o)$. For a fixed flow rate, Q_o, increasing the volume fraction of particles (ν_p) requires a corresponding increase in the pressure differential. Explicitly, the Reynolds number is

$$\mathcal{R}_{ec} = \frac{v_{max} D \rho^*}{\mu^*} = \frac{2Q_o(q+2)}{\pi R q} \frac{((1-\nu_p)\rho_f + \nu_p \rho_p)}{\mu_f(1 + 2.5\frac{\nu_p}{1-\nu_p})}. \tag{7.11}$$

Fig. 3 shows the dependency of the Reynolds number on the volume fraction, using the previous simulation parameters and profile constants: $c_1 = 0.01$ and $c_2 = 2$. For the case considered, for increasing volume fraction, the profile changes (blunts) moderately to approximately $q = c_1 \mathcal{R}_{ec} + c_2 \approx 3$, then decreases due to the increased effective viscosity. However, while these models can provide macroscopic quantitative and qualitative information, more detailed microscale information on the flow requires complex spatio-temporal discretization resolving multiparticle particle-fluid interaction. Such particle-fluid systems are strongly coupled, due to the drag forces induced by the fluid onto the particles and vice-versa. For example, in Zohdi (2014), a flexible and robust solution strategy was developed to resolve coupled systems comprised of large groups of flowing charged particles embedded within a continuous fluid, based on numerical iterative schemes to resolve the coupling. The approach can be used in conjunction with computational fluid mechanics codes based on finite difference, finite element, finite volume or discrete element discretization and is under further development to characterize electrically-functionalized fluid systems is under by the author.

Supplementary material

Supplementary material associated with this article can be found, in the online version, at 10.1016/j.ijengsci.2017.11.003.

References

Ahmad, Z., Rasekh, M., & Edirisinghe, M. (2010). Electrohydrodynamic direct writing of biomedical polymers & composites. *Macromolecular Materials & Engineering, 295*, 315–319.

Avci, B., & Wriggers, P. (2012). A DEM-FEM coupling approach for the direct numerical simulation of 3d particulate flows. *Journal of Applied Mechanics, 79*(010901), 1–7.

Choi, S., Jamshidi, A., Seok, T. J., Zohdi, T. I., Wu. , M. C., & Pisano, A. P. (2012). Fast, high-throughput creation of size-tunable micro, nanoparticle clusters via evaporative self-assembly in picoliter-scale droplets of particle suspension. *Langmuir, 28*(6). 3102-11

Choi, S., Park, I., Hao, Z., Holman, H. Y., Pisano, A. P., & Zohdi, T. I. (2010a). Ultra-fast self-assembly of micro-scale particles by open channel flow. *Langmuir, 26*(7), 4661–4667.

Choi, S., Pisano, A. P., & I. , Z. T. (2013). An analysis of evaporative self-assembly of micro particles in printed Picoliter suspension droplets. *Journal of Thin Solid Films, 537*(30), 180–189.

Choi, S., Stassi, S., Pisano, A. P., & Zohdi, T. I. (2010b). Coffee-Ring effect-Based three dimensional patterning of micro, nanoparticle assembly with a single droplet. *Langmuir, 26*(14), 11690–11698.

Demko, M. T., Cheng, J. C., & Pisano, A. P. (2010). High-resolution direct patterning of gold nanoparticles by the microfluidic molding process. *Langmuir*, 412–417.

Demko, M. T., Choi, S., Zohdi, T. I., & Pisano, A. P. (2012). High resolution patterning of nanoparticles by evaporative self-assembly enabled by in-situ creation & mechanical lift-off of a polymer template. *Applied Physics Letters, 99*. 253102-1-253102-3

Einstein, A. (1906). A new determination of molecular dimensions. *Annals of Physics, 19*(4), 289–306.

Hashin, Z. (1983). Analysis of composite materials: A survey. *ASME Journal of Applied Mechanics, 50*, 481–505.

Hashin, Z., & Shtrikman, S. (1962). On some variational principles in anisotropic & nonhomogeneous elasticity. *Journal of the Mechanics & Physics of Solids, 10*, 335–342.

Hashin, Z., & Shtrikman, S. (1963). A variational approach to the theory of the elastic behaviour of multiphase materials. *Journal of the Mechanics & Physics of Solids, 11*, 127–140.

Hinze, J. O. (1975). *Turbulence*. McGraw-Hill. New York.

Kachanov, M., & Abedian, B. (2015). On the isotropic & anisotropic viscosity of suspensions containing particles of diverse shapes & orientations. *International Journal of Engineering Science, 94*, 71–85.

Leonardi, A., Wittel, F. K., Mendoza, M., & Herrmann, H. J. (2014). Coupled DEM-LBM method for the free-surface simulation of heterogeneous suspensions. *Computational Particle Mechanics, 1*(1), 3–13.

[2] In the special case of laminar flow ($c_1 = 0$ and $c_2 = 2$) there are two roots to Eq. (7.9), $q = 2$ and $q = 0$.

Martin, P. (2009). *Handbook of deposition technologies for films & coatings* (3rd ed.). Elsevier.
Martin, P. (2011). *Introduction to surface engineering & functionally engineered materials*. Scrivener & Elsevier.
Onate, E., Celigueta, M. A., Latorre, S., Casas, G., Rossi, R., & Rojek, J. (2014). Lagrangian analysis of multiscale particulate flows with the particle finite element method. *Computational Particle Mechanics, 1*(1), 85–102.
Park, I., Ko, S. H., Pan, H., Grigoropoulos, C. P., Pisano, A. P., Frechet, J. M. J., et al. (2008). Nanoscale patterning & electronics on flexible substrate by direct nanoimprinting of metallic nanoparticles. *Advanced Materials, 20*, 489.
Park, J. U., Hardy, M., Kang, S. J., Barton, K., Adair, K., Mukhopadhyay, D. K., et al. (2007). High-resolution electrohydrodynamic jet printing. *Nature Materials, 6*, 782–789.
Probstein, R. (2003). *Physiochemical hydrodynamics: An introduction* (2nd ed.). Wiley.
Samarasinghe, S. R., Pastoriza-Santos, I., Edirisinghe, M. J., Reece, M. J., & Liz-Marzan, L. M. (2006). Printing gold nanoparticles with an electrohydrodynamic direct write device. *Gold Bulletin, 39*, 48–53.
Sevostianov, I., & Kachanov, M. (2012). Effective properties of heterogeneous materials: Proper application of the non-interaction & the “dilute limit” approximations. *The International Journal of Engineering Science., 58*, 124–128.
Torquato, S. (2002). *Random heterogeneous materials: Microstructure & macroscopic properties*. New York: Springer-Verlag.
Zohdi, T. I. (2014). Embedded electromagnetically sensitive particle motion in functionalized fluids. *Computational Particle Mechanics, 1*, 27–45.
Zohdi, T. I., & Wriggers, P. (2008). *Introduction to computational micromechanics*. Springer-Verlag.